Published in final edited form as:

Matrix Biol. 2019 September ; 82: 71–85. doi:10.1016/j.matbio.2019.03.002.

Thrombospondin-2 regulates extracellular matrix production, LOX levels, and cross-linking via downregulation of miR-29

N.E. Calabro[a,b], **A. Barrett**[e], **A. Chamorro-Jorganes**[a,d], **S. Tam**[a], **N.J. Kristofik**[f], **Xing Hao**[a], **Ayomipose M. Loye**[a,f], **W.C. Sessa**[a,c], **K. Hansen**[e], **T.R. Kyriakides**[a,b,f]

[a]-Interdepartmental Program in Vascular Biology and Therapeutics, Yale University School of Medicine, New Haven, CT 06510, USA

[b]-Department of Pathology, Yale University School of Medicine, New Haven, CT 06510, USA

[c]-Department of Pharmacology, Yale University School of Medicine, New Haven, CT 06510, USA

[d]-Department of Comparative Medicine, Yale University School of Medicine, New Haven CT 06510, USA

[e]-Department of Biochemistry and Molecular Genetics, and ‡Biological Mass Spectrometry Facility, University of Colorado Denver, Aurora, CO 80045, USA

[f]-Department of Biomedical Engineering, School of Engineering and Applied Science, Yale University, New Haven, CT 06511, USA

Abstract

Collagen fibrillogenesis and crosslinking have long been implicated in extracellular matrix (ECM)-dependent processes such as fibrosis and scarring. However, the extent to which matricellular proteins influence ECM protein production and fibrillar collagen crosslinking has yet to be determined. Here we show that thrombospondin 2 (TSP2), an anti-angiogenic matricellular protein, is an important modulator of ECM homeostasis. Specifically, through a fractionated quantitative proteomics approach, we show that loss of TSP2 leads to a unique ECM phenotype characterized by a significant decrease in fibrillar collagen, matricellular, and structural ECM protein production in the skin of TSP2 KO mice. Additionally, TSP2 KO skin displays decreased lysyl oxidase (LOX), which manifests as an increase in fibrillar collagen solubility and decreased levels of LOX-mediated fibrillar collagen crosslinking. We show that these changes are indirectly mediated by miR-29, a major regulator of ECM proteins and LOX, as miR-29 expression is increased in the TSP2 KO. Altogether, these findings indicate that TSP2 contributes to ECM production and assembly by regulating miR-29 and LOX.

Correspondence to Themis R. Kyriakides: T.R. Kyriakides, Department of Pathology, Yale University School of Medicine, 10 Amistad Street, Room 301C, New Haven, CT 06520, USA. themis.kyriakides@yale.edu.

Keywords

extracellular matrix; thrombospondin 2; collagen; proteomics; lysyl oxidase; miR-29

Introduction

The extracellular matrix (ECM) is a dynamic, collagenous network necessary for maintaining bodily structure and stability [1]. Comprised of collagens, fibronectin, laminin, matricellular proteins, proteoglycans, and other components, the ECM serves as a regulatory substrate that allows for cellular attachment, along with modulation of cell signaling and cellular behavior [2]. ECM assembly is influenced by secreted enzymes such as matrix metalloproteinases (MMPs) and cross-linking enzymes such as lysyl oxidase (LOX) which help to maintain an ideal, balanced organization and composition through post-translational modifications [3, 4] [5, 6]. Downregulation of LOX in vitro leads to disordered collagen fibrillogenesis[7], while loss of LOX in mice causes perinatal death due to lack of elastin and collagen fiber integrity[8]. MicroRNAs, particularly miR-29, also contribute to maintaining its homeostasis through negatively regulating ECM protein production [9–15]. miR-29 has known and predicted targeting sites on the transcripts for collagens, LOX, and various ECM proteins, with downregulation of miR-29 contributing to development of pulmonary and liver fibrosis[10, 16]. Disorders characterized by disruption of collagen, elastin, or fibrillin-1, such as Ehlers-Danlos Syndrome (EDS), Williams-Beuren Syndrome, and Marfan Syndrome are hallmarked by a laxity in skin, connective tissue disorder, and predisposition for aortic aneurysms due to compromised ECM integrity [17–19]

Matricellular proteins are non-structural components of the ECM that contribute to proper ECM assembly and organization. Additionally, matricellular proteins influence cellular behavior through interaction with cell surface receptors, collagens, proteases, and sequestration of growth factors [20, 21]. Thrombospondins are of particular interest due to their role in modulating angiogenesis, collagen fibrillogenesis, and coagulation [22–24]. TSP1 and TSP2, the most studied members of the thrombospondin family, have high sequence homology yet distinct secretion and functions [25]. TSP1, secreted by platelets, activates latent TGF-B[26] and inhibits angiogenesis through binding cell surface receptors such as CD36 and CD47[27, 28]. TSP1 KO mice display increased vascular density, thoracic kyphosis, and pulmonary inflammation, with TSP1 dictating the course of dermal wound healing [29]. A recent study described a direct interaction between TSP1 and LOX and reduced collagen content in TSP1 KO mice but their phenotype does not reflect significant issues with ECM assembly and homeostasis[30]. Unlike TSP1 KO mice, TSP2 KO mice exhibit an ECM-centric phenotype characterized by bleeding diathesis, increased vascular density, and connective tissue disorder associated with abnormal collagen fibrils [31]. Specifically, it was found that TSP2 KO mice exhibit irregular collagen fibrils with a non-homogenous distribution of shape, size, and organization. Subsequently, these abnormalities lead to the formation of disorganized fibers that lacked the classic parallel alignment seen in WT skin. Collectively, these changes result in increased skin laxity and decrease in tensile strength.

Aside from collagen, TSP2 influences other proteins in the extracellular environment as well, particularly in the context of ECM remodeling. MMP-2 is of great interest, as it cleaves fibrillar collagens near the N-terminus of the protein[32], producing gelatin that can be further degraded by MMP-9 [33]. TSP2 has been demonstrated to directly bind MMP-2 [34], targeting the enzyme for degradation via LRP1 [35]. In environments lacking TSP2, both MMP-2 and MMP-9 levels are significantly higher, as TSP2 is not present to assist in recycling these enzymes. Because of this, the ECM is more highly degraded, leading to exposure of cryptic collagen epitopes [36]. Along with increased ECM degradation, it was also determined that tTG (tissue transglutaminase) activity is lower in TSP2 KO mice. Specifically, it was found that tTG is a proteolytic target of MMP-2, and because of this, tTG activity is significantly impaired. This change in tTG activity leads to the formation of fewer isopeptide crosslinks, contributing to the ECM abnormalities observed in TSP2 KO mice [37].

As past findings have highlighted the need to further examine the collagenous phenotypic changes in TSP2 KO mice, we initiated studies to investigate the role TSP2 plays in ensuring proper ECM balance. Quantitative proteomic analysis of WT and TSP2 KO skin revealed a decrease in fibrillar collagen levels within TSP2 KO skin, along with surprising decreases in various matricellular and structural ECM proteins. Furthermore, quantitative HPLC analysis highlighted significant decreases in divalent and trivalent fibrillar collagen crosslinks, explaining the increased collagen solubility seen in TSP2 KO skin. Upon closer examination, it was found that this decrease in fibrillar collagen crosslinking was due to unexpectedly lower levels of LOX in TSP2 KO skin. Finally, it was determined that miR-29 levels are increased in a TSP2 KO environment, which could potentially contribute to altered levels of ECM protein production. Upon rescue via transfection of pcDNA TSP2 into TSP2 KO dermal fibroblasts (DF), it was found that both LOX and miR-29 reached WT levels. Moreover, treatment of TSP2 KO DF with anti-miR-29 caused an increase in LOX. Collectively, these findings highlight a novel axis involving TSP2, LOX, and miR-29 in which TSP2 within the extracellular environment helps to maintain appropriate levels of these molecules, ensuring proper ECM composition, assembly, and integrity.

Results

TSP2 KO skin exhibits a unique ECM profile highlighted by decreased fibrillar collagen, matricellular, and structural protein levels.

Quantitative LC-MS/MS proteomics using QconCAT protein standards and a multi-step fractionation/digestion protocol [38, 39] was used to examine the protein composition of WT and TSP2 KO adult skin. Analysis of WT and TSP2 KO skin from 12–16 week-old mice revealed significant decreases in numerous ECM and ECM related proteins (Table S1). Overall, 41 proteins were quantified with a significant change observed in 17 proteins (Table S2). Of note, both collagen Iα1 and Iα2 chains were significantly decreased in TSP2 KO skin, highlighting an overall fibrillar collagen deficiency.

Multivariate analysis of this data revealed that TSP2 KO skin possessed a unique ECM protein profile as evidenced by the distinct clustering of WT and TSP2 KO samples within the PLS-DA plot (Fig. 1A). Excitingly, TSP2 KO skin contained significantly less fibrillar

collagens, as demonstrated by decreases in collagen Iα1, Iα2, and collagen V (Fig. 1B, C). Additionally, it was found that collagen associated matricellular proteins including lumican, collagen VI, and dermatopontin were significantly decreased in TSP2 KO skin (Fig. 1D), along with collagen associated structural ECM proteins fibrillin-1, decorin, and biglycan (Fig. 1E). However, there was no global decrease in ECM proteins, as levels of major basement membrane proteins collagen IV and laminin (Fig. 1F), along with matricellular proteins that are not closely associated with collagen, such as prolargin, tenascin, and periostin (Fig. 1G) were similar between WT and TSP2 KO skin. Additionally, despite changes in some protein levels within TSP2 KO skin, the hierarchy of protein abundances remained similar (Fig. S1). Taken together, these findings highlight a decrease of fibrillar collagens, structural ECM proteins, and matricellular proteins in TSP2 KO skin, with no resultant effect on global protein levels.

TSP2 KO skin displays increased fibrillar collagen and structural ECM protein solubility.

Due to irregular collagen fibrillogenesis and organization, TSP2 KO skin is characterized by an abnormal skin laxity and decrease in tensile strength [31]. As increases in skin laxity can be attributed to increases in protein solubility, we sought to examine the solubility profile of TSP2 KO skin across cellular, soluble ECM (sECM), and insoluble ECM (iECM) fractions. Cellular fractions were generated by skin homogenization in CHAPS buffer. sECM fractions were collected after 6M urea treatment and iECM fractions were obtained after a final treatment with CNBr. There was no difference in solubility patterns amongst protein classes between WT and TSP2 KO skin (Fig. S2A,B). Upon examination of each separate fraction, solubility did not differ within the cellular fraction (Fig 2A), but TSP2 KO skin demonstrated a 11.9% increase of soluble fibrillar collagens within the sECM fraction (Fig. 2B,D). The increase of fibrillar collagens in the sECM fraction was associated with a corresponding decrease in the iECM fraction (Fig. 2C). A similar pattern was observed with the structural ECM protein class (Fig. 2B,C). Specific to fibrillar collagen, in the cellular fraction WT and TSP2 KO samples contained 3.0 ± 0.6 and 4.4 ± 0.8%, respectively (pvalue 0.07). In the sECM fraction, WT contained 44.6 ± 7.5% and TSP2 KO 56.5 ± 8.3% (pvalue 0.0021)> Finally, in the iECM fraction, WT containd 52.4 ± 9.2% and TSP2 KO 56.5 ± 39.1% (pvalue 0.0026). A complete list of solubility levels across fractions can be found Fig. S2B. Overall, these results demonstrate enhanced fibrillar collagen solubility in TSP2 KO skin which could be due to defects in ECM crosslinking and assembly defect.

Lack of TSP2 leads to a collagen crosslinking defect in skin.

Beyond examining isopeptide crosslink levels [37], no quantified characterization of collagen crosslinking has been performed in TSP2 KO skin. Based on the fibrillar collagen solubility findings, it could be hypothesized that there is insufficient collagen crosslinking in TSP2 KO skin. In order to test this hypothesis, HPLC was employed to examine major divalent and trivalent collagen crosslinks in WT and TSP2 KO skin. Interestingly, in comparison to WT, TSP2 KO skin demonstrated a significant decrease in divalent crosslinks, LNL and DHLNL, (Fig. 3 A,B) and trivalent crosslink pyridinoline (Pyr) (Fig. 3C). Additionally, the peroxidasin mediated collagen IV crosslink sHLM was decreased (Fig. 3D). Taken together, these changes result in a decrease in total crosslinks in TSP2 KO skin (Fig. 3E). However, there was not a global defect in crosslinks as HLNL and HHMD were

not significantly decreased (Fig. 3 F,G). Combined, these data indicate that there is an overall decrease in fibrillar collagen crosslinking, leading to an increase in fibrillar collagen solubility.

Lack of TSP2, both in vivo and in vitro, leads to a decrease in LOX.

LOX is the major extracellular fibrillar collagen crosslinking enzyme that mediates the progression from fibrils to fibers and it is integral in maintaining ECM organization and mechanical stability [40]. As we found TSP2 KO skin exhibits less total collagen crosslinks, particularly fibrillar collagen crosslinks, it was hypothesized that loss of TSP2 leads to decreased LOX. In order to probe this hypothesis, we first examined LOX levels under ECM producing conditions *in vitro*. Dermal fibroblasts are the predominant cell type that produces both TSP2 and fibrillar collagens *in vivo* [41]. Because of this, dermal fibroblasts were isolated from WT and TSP2 KO mice and cultured with ascorbic acid in order to stimulate active ECM deposition. At days 3 and 7 in culture, cells were collected and LOX levels were examined via Western blot. At both timepoints, LOX (pro-form) was significantly lower in the TSP2 KO cells, as quantified by densitometry (Fig. 4A). Decreased LOX was also observed in conditioned media of TSP2 KO cells (Fig. S3) Examination of the expression of other cross-linking enzymes, including LOXL1, revealed no differences between WT and TSP2 KO DF (Fig. S4). We also observed reduced LOX mRNA in TSP2 KO cells at day 3 (Fig. S5A). In order to examine LOX production in an active ECM producing environment *in vivo*, full-thickness dermal wounds were harvested from WT and TSP2 KO mice at days 7 and 10 post-wounding and stained for LOX via IHC. Consistent with *in vitro* findings, wounds from TSP2 KO mice display decreased LOX staining in comparison to WT (Fig. 4B). Together, these findings highlight that LOX correlates with TSP2 levels in actively producing ECM conditions, both *in vitro* and *in vivo*.

miR-29 levels are increased in TSP2 KO DF.

miR-29 has known and predicted targeting sites on numerous ECM proteins and has been shown to negatively regulate many ECM proteins including collagens and LOX [10, 12, 13, 15, 42]. Due to the abnormal collagen phenotype and decrease in LOX levels in TSP2 KO mice, it was hypothesized that miR-29 levels might be altered in TSP2 KO DF. In order to further investigate this hypothesis, WT and TSP2 KO DF were treated with ascorbic acid and day 3 and 7 timepoints were collected to examine miR-29 levels. qPCR analysis revealed that all miR-29 family members were increased at days 3 and 7 in TSP2 KO DF compared to WT (Fig. 5A, B). Other miRs including let-7a, miR-19b, and miR-30c have been implicated in ECM regulation, with let-7a, miR-19b, and miR-30c downregulation leading to excessive collagen production [11, 43, 44]. In order to determine if these ECM-related miRs are also altered in TSP2 KO cells, expression was measured in the same samples listed above. Interestingly, levels of these miRs were not decreased in TSP2 KO compared to WT (Fig. S6). Overall these findings indicate that increased miR-29 is associated with altered collagen and LOX levels in TSP2 KO DF, but that there is not a global change in ECM-related miRs.

TSP2 in TSP2 KO DFs influences LOX and miR-29 levels.

No direct link is known to exist between TSP2 and LOX or TSP2 and miR-29. As loss of TSP2 was shown to decrease collagen and LOX protein and increase miR-29 levels, it was hypothesized that reintroduction of TSP2 into TSP2 KO DF would modulate their levels to near those in WT. To probe this hypothesis, TSP2 KO cells were transfected with either empty vector pcDNA or pcDNA TSP2 and RNA and protein lysates were collected at 48 hours post-transfection. As seen in Fig. 6A, TSP2 production in TSP2KO DF resulted in an increase in LOX protein levels. In addition, LOX mRNA was increased (Fig. S5B). Transfection of TSP2 KO cells also modulated miR-29 levels, as rescue of TSP2 led to a decrease in expression of the miR-29 family (Fig. 6B). We did not observe a change in Col1 levels within the 48 hour experimental window. This could be due to the short duration of transfection and/or the existence of additional regulators of collagen synthesis. In addition, transfection of LNA-miR-29 in TSP2 KO DF reduced miR-29 levels resulting in an increase in LOX protein (Fig. 6C) and mRNA (Fig. S5C). To control for non-specific LNA effects on protein production, in independent experiments we used GAPDH or HSP90 to detect loading. These findings highlight an integral role for TSP2 in modulating two very important ECM regulators.

Discussion

Previous work examining the collagen phenotype in TSP2 KO mice has demonstrated that loss of TSP2 leads to connective tissue abnormalities consequent of disordered collagen fibrillogenesis and assembly [31]. Here, we further characterize this altered collagen phenotype by demonstrating that loss of TSP2 has a profound impact not only on collagen assembly, but also on ECM protein composition and collagen crosslinking. Past studies have implicated TSP2 in influencing the collagen I content in ECM produced by mesenchymal stromal cells undergoing osteoblastic differentiation [45] and demonstrated that it affects collagen I incorporation into bone [46]. However, no studies have been performed that examine the extent to which collagen I levels, along with other ECM proteins, are affected by loss of TSP2.

Fractionation of tissue samples into cellular, soluble ECM, and insoluble ECM fractions allows for a comprehensive analysis of tissue solubility, protein content, and profile [38]. Here, quantitative proteomic analysis was used in order to determine the amounts of various proteins within skin. Excitingly, these studies demonstrated a decrease in both collagen Iα1 and collagen Iα2, along with a decrease in collagen V in TSP2 KO skin. Collagen V is closely associated with collagen I as it forms heterotypic fibrils with collagen I, serving a regulatory role in modulating collagen I nucleation and fibrillogenesis [47, 48].

Aside from the decreased fibrillar collagen levels in TSP2 KO skin, there was also a corresponding decrease in matricellular and structural ECM proteins. Specifically, matricellular proteins lumican, collagen VI, and dermatopontin were decreased in TSP2 KO skin. Lumican has been shown to regulate collagen fibril assembly [49], collagen VI forms beaded microfilaments that directly bind to collagen I [50], and dermatopontin plays a role in collagen fibrillogenesis and fibril orientation [51]. Structural ECM proteins fibrillin-1, decorin, and biglycan were also decreased in TSP2 KO skin. Decorin and biglycan are

closely related proteoglycans which bind collagen fibrils, modulating tissue development and assembly [52–54]. Not all matricellular proteins were decreased in TSP2 KO skin however. Prolargin, tenascin, and periostin levels were similar between WT and TSP2 KO skin. These proteins do not directly associate with collagen I. Additionally, levels of basement membrane proteins collagen IV and laminin were similar. Overall, the analysis revealed changes in fibrillar collagens or associated molecules. Matricellular and structural ECM proteins that associate with collagen I and regulate fibrillogenesis were decreased in TSP2 KO skin. The lack of change in other matricellular proteins and basement membrane proteins indicate that the changes in TSP2 KO skin are predominantly associated with fibrillar and structural ECM components.

Findings regarding fibrillar collagen solubility are intriguing, especially in the context of decreased LOX levels, as they expand on and validate past studies that focused on basic urea extraction in TSP2 KO skin. Increased fibrillar collagen solubility implies lower levels of collagen cross-linking, specifically those crosslinks mediated by LOX [40]. Lower LOX levels in both TSP2 KO skin and ECM is surprising, as few studies exist demonstrating a link between matricellular proteins and LOX with the exception of either TSP1 or fibulin-4 in modulating LOX through direct interaction with the enzyme [30, 55, 56]. Moreover, fibulin-4 KO mice display changes in collagen fibrillogenesis in bone that are associated with reduced LOX levels [57].

Knockout of LOX leads to a perinatal lethal phenotype characterized by impaired development of the cardiovascular system and aortic aneurysms [58, 59]. Decrease in LOX levels or activity is known to result in impaired collagen fibrillogenesis [7] and significant lack of crosslinking, leading to lathyrism and fragile skin [60], while over production of LOX expedites cardiac remodeling [61] and is associated with fibrotic phenotypes [62]. All of these findings highlight the integral role of LOX in maintaining crosslink homeostasis and tissue structural integrity. It is no surprise then that due to a decrease in LOX, there is a corresponding reduction of LOX-mediated collagen crosslinks in TSP2 KO skin. Specifically, decreases in immature divalent LNL and DHLNL and mature trivalent pyridinoline crosslinks contribute to the overall total decrease of crosslinks in TSP2 KO skin. sHLM, the only known collagen IV crosslink [63], was also determined to be lower in TSP2 KO skin. sHLM formation is not mediated by LOX, rather, it is catalyzed by peroxidasin, a H_2O_2 dependent enzyme that forms sulfilimine bonds [64, 65]. H_2O_2 is a byproduct of LOX's reaction with cofactor LTQ during formation of reactive aldehydes on collagen or elastin [66]. As there is less LOX in the TSP2 KO environment, perhaps there is also less generation of H_2O_2 and reactive oxygen species, thus dampening peroxidasin's enzymatic activity and leading to a decrease in collagen IV crosslinking.

Dysregulation of miR-29 levels has been implicated in numerous pathological conditions involving alterations in collagen deposition. Specifically, miR-29 is downregulated in systemic sclerosis, and many fibrotic conditions [15, 67, 68]. Inhibition of miR-29 successfully stabilizes atherosclerotic plaques through an increase in ECM deposition [69] and increases elastin levels in conditions of elastin haploinsufficiency [42]. Here we show that loss of TSP2 influences miR-29 expression highlighting the diverse roles that matricellular proteins can play in maintaining ECM signaling and homeostasis. Based on

these observations, we hypothesized that TSP2 indirectly modulates miR-29 through influencing negative regulators of miR-29, either pre- or post-transcriptionally. In order to determine if miR-29 regulation occurs at the transcriptional level, expression of miR-29a primary transcript was examined. qPCR analysis of day 3 and day 7 samples revealed no differences in pri-miR-29 expression between WT and TSP2 KO (Fig. S7). These results indicate that TSP2 does not modulate miR-29 pre-transcriptionally.

Production of exogenous TSP2 in TSP2 KO cells led to increased and decreased LOX and miR-29, respectively. In addition, targeting the excess miR-29 in TSP2 KO DF with an anti-miR resulted in an increase in LOX. These findings indicate that TSP2 influences miR-29 expression and via this effect, indirectly regulates LOX.

While other studies have implicated matricellular proteins in participating in the maintenance of ECM homeostasis through direct binding of ECM proteins or modifying enzymes, this is the first study to comprehensively and quantitatively demonstrate that loss of a matricellular protein leads to an ECM assembly defect associated with an overall decrease in collagenous, structural, and matricellular proteins *in vivo*. Additionally, this study shows quantitatively that multiple divalent and trivalent LOX-mediated collagen crosslinks are decreased in the TSP2-KO environment *in vivo* and that the delicate balance between proper ECM content, assembly, and crosslinking is lost. LOX and miR-29 appear to be key players in modulating this altered ECM phenotype as levels of both are changed upon loss of TSP2. Collectively, these findings demonstrate a novel link between TSP2, collagen, LOX, and miR-29 that is regulated by the presence or absence of TSP2 in the extracellular environment, forming a feedback loop between cells and its ECM substrate (Fig. 7).

Experimental Procedures:

Mouse Strains and Care

TSP2 KO mice were generated as previously described [31]. Male mice aged 12–16 weeks were used for all experiments. Mice were kept under constant temperature and humidity in a 12 hour controlled dark/light cycle. All experiments were approved by the Institutional Animal Care Use Committee of Yale University School of Medicine.

Quantitative Proteomics

The following protocol was adapted from [38, 39, 70]. Briefly, skin samples from WT and TSP2 KO mice were homogenized in CHAPS buffer and sequentially extracted using high speed centrifugation in CHAPS, 6M urea, and CNBr, resulting in cellular, soluble ECM, and insoluble ECM fractions. Fractions were then spiked with QconCAT standards at 100 fmol 13C6 QconCAT/5 μg protein and trypsin digested, with equal volumes per fraction loaded for analysis via LC-MS/MS (LTQ Orbitrap Velos, Thermo). Data was processed as described previously [70]. Gene annotations were determined using the Database for Annotation, Visualization, and Integrated Discovery (DAVID) [71]. Multivariate statistical analysis was performed using the MetaboAnalyst supervised classification method of partial least squares - discriminant analysis (PLS-DA). Cross-validation and permutation tests were used to establish statistical significance ($P < 0.05$) as reported [72, 73]. Solubility as reported

in figure 2A-C, was calculated from the target proteomics data using the sum of peptide peak areas for proteins within each of the six protein categories divided by total signal across all fractions. Cellular values are based on MS data resulting from the CHAPS extraction and soluble ECM and insoluble ECM likewise resulted from MS data from 6M urea and CNBr fractions respectively.

Crosslink Analysis

The following protocol was adapted from Sims et al [74]. Briefly, skin samples (approximately 5 mg) from WT and TSP2 KO mice underwent NaBH4 reduction (conc, 25 °C, 1 hour), followed by hydrolysis in neat hydrochloric acid (100 °C, 24hours, sealed glass vessel), lyophilization to dryness under vacuum, and rehydrated in 0.1% formic acid solution. Hydroxyproline content was determined by running a 1:10 dilution of the pre-enrichment sample by positive ion mode MS on the QExactive mass spectrometer as previously reported [75]. The cross-linked amino acids were measure by a MRM targeted MS method with pre-enrichment on cellulose resin (CF11, Whatman) as reported [76]. Normalization of cross-linked amino acid peak areas was performed using hydroxyproline and tissue dry weight pre-hydrolysis. Statistical analysis, including t-test and ANOVA (significance threshold for P values <0.05) were performed on normalized peak areas. Total cross-link plots were generated by summing normalized peak areas for all cross-links in a specific sample.

Primary Dermal Fibroblast Isolation and Culture

WT and TSP2 KO DF were isolated from skin using a collagenase and trypsin digestion protocol. Briefly, mice aged 3–4 months were sacrificed via CO2 chamber. Upon confirmation of death, skins were excised from the dorsal region of the mice and washed in DMEM (Gibco). Skins were then treated for 15 minutes in antibiotic solution containing 20% pen/strep, 3% amphotericin B (Sigma), and DMEM. After antibiotic treatment, skins were transferred to a trypsin overnight incubation solution containing 0.25% Type IX-S porcine pancreas trypsin (Sigma), 1.5% pen/strep, 1.5% amphotericin B, and DMEM, and left to digest overnight at 4℃. Upon completion of trypsin digestion, the subdermal fat was removed and the dermis was cut into small pieces. The dermis was then placed in a collagenase digestion solution containing 0.25% type IV collagenase (Worthington) and DMEM, and left to digest for approximately 3–5 hours. Upon complete digestion, DFs were collected by multiple centrifugations and plated in tissue culture dishes at 37℃/5% CO2 in DMEM supplemented with 10% FBS, 100 g/ml streptomycin, 100U/ml penicillin (Gibco), and amphotericin B (Sigma). For cultures stimulated to produced ECM, cells were supplemented with 50 uM ascorbic acid (Alfa Aesar) for every other day grown in culture.

Full Thickness Dermal Wounds and Immunohistochemistry

WT and TSP2 KO mice were given full thickness dermal wounds using biopsy punches as previously described [77]. Briefly, mice were anesthetized with isofluorane and excisional wounds were made using a 6mm biopsy punch. At day 7 post wounding, wounds were harvested, fixed in 10% formalin, and embedded in paraffin. Five micrometers of tissue were sectioned per slide. Samples were deparaffinized at 55°C for 40 minutes, treated with xylene (J.T. Baker), and rehydrated in 100% and 95% ethanol (Decon). Slides were then subjected

to a peroxidase block (3% H2O2/0.1% sodium azide/MeOH) for 30 minutes and blocked in 1% BSA/PBS for 30 minutes. Primary LOX antibody (Abcam; Ab31238) was used at a 1:100 dilution and incubated at 4°C overnight. Secondary antibody, anti-rabbit HRP, was added at a dilution of 1:200 and incubated at room temperature for 30 minutes. ABC reagent (Vector) was incubated for 30 minutes, and then DAB solution (Vector) was added to slides for 2 minutes. Samples were counterstained in methylene green, dehydrated in a series of ethanol and xylene washes, and coverslips were mounted.

Plasmids and Transfection

Control mouse pcDNA3.1 empty vector and pcDNA3.1 mTSP2 constructs were purchased from Addgene. DF were transfected with 0.5 μg of pcDNA3.1 empty vector or pcDNA3.1 mTSP2 using Lipofectamine LTX with Plus (Invitrogen) following manufacturer's protocol for 48 hours. LNA-anti-miR-29 and LNA-CTL oligos were used as described previously [69]. Briefly, TSP2-KO DF were transfected with 100 nM LNA-anti-miR-29 and LNA-CTL using Lipofectamine™ RNAiMAX (Invitrogen) according to the supplier's instructions. RNA and proteins were isolated 24 hrs and 48 hrs post-transfection, respectively.

Quantitative Real-Time PCR analysis

miRNA qPCR: RNA was isolated from DF using miRNeasy Mini Kit (Qiagen) according to manufacturer's protocol. Up to 1 μg RNA was reverse transcribed using the miScript II RT Kit (Qiagen) according to manufacturer's protocol. Quantitative real-time PCR was performed using Quantitect SYBR Green PCR Kit (Qiagen) according to manufacturer's protocol. Mouse miR-29 a/b/c, let-7, miR-19b, miR-21, miR-30, and miR-145 were purchased from Qiagen (miScript primer assays #218300-MS00001372, MS00005936, MS00001379, MS00010983, MS000218300, MS00011487, MS00001631). Snord68 (MS00033712) was used as a housekeeping gene. Primers for qPCR were synthesized by Keck Center at Yale (see Supplemental Table 3 for specific sequences). pri-miRNA qPCR: RNA was isolated as described above. cDNA was synthesized using the TaqMan RT Kit (Applied Biosystems) according to manufacturer's protocol. Quantitative real-time PCR was performed using TaqMan Universal Master Mix (Applied Biosystems), examining pri-mir-29a (Mm03306859_pri) and housekeeping gene 18s (Hs03003631_g1).

Western Blot analysis

Cells were lysed in ice-cold buffer containing 50 mM Tris-HCl, pH 7.5, 125 mM NaCl, 1% NP-40, 5.3 mM NaF, 1.5 mM NaP and 1mM orthovanadate, 175 mg/ml octylglucopyranoside, 1 mg/ml of protease inhibitor coctail (Roche), and 0.25 mg/ml 2 AEBSF (Roche). Cell lysates were rocked at 4°C for 45 minutes before the insoluble material was removed by centrifugation at 12,000 × g for 15 min. After normalizing for equal protein concentration, cell lysates were resuspended in SDS sample buffer (between 10 μg-30 μg protein used) and run on a 10% SDS-PAGE gel. Proteins were transferred onto 0.22 μm nitrocellulose membrane and blocked with 3% BSA. Western blots were performed using the following antibodies: TSP2 (1:250, BD), LOX (1:100, Abcam, Ab31238 detects both the pro-peptide and active/mature LOX), LOXL1 (1:500, Abcam, Ab81488), HSP90 (1:1000, Santa Cruz), Collagen I (1:500, Abcam), GAPDH (1:2000, Cell Signaling 21185). Protein bands were visualized using the Odyssey Infrared Imaging System (LICOR

Biotechnology). Densitometry analysis of the gels was carried out using NIH ImageJ software (http://rsbweb.nih.gov/ij/).

Statistical Analysis

Data are expressed as mean ± SEM. Statistical differences were measured by student t-test. A value of $p \leq 0.05$ was considered statistically significant. Data analysis was performed using Prism (GraphPad).

Supplementary Material

Refer to Web version on PubMed Central for supplementary material.

Acknowledgements

This work was supported by the National Institutes of Health (grant numbers HL 107205 to T.R.K, W.C.S and GM-072194 to T.K.)

Abbreviations:

TSP2	thrombospondin 2
LOX	lysyl oxidase
MMP	matrix metalloproteinase
TSP1	thrombospondin 1
tTG	tissue transglutaminase
COL	collagen
LUM	lumican
DPT	dermatopontin
FBN1	fibrillin-1
DEC	decorin
BGN	biglycan
LAMB2	laminin b2
PRELP	prolargin
TNC	tenascin-c
POSTN	periostin
TGFBI	TGFB induced

References

[1]. Iozzo RV, Gubbiotti MA, Extracellular matrix: The driving force of mammalian diseases, Matrix Biol 71–72 (2018) 1–9.

[2]. Frantz C, Stewart KM, Weaver VM, The extracellular matrix at a glance, J Cell Sci 123(Pt 24) (2010) 4195–200. [PubMed: 21123617]

[3]. Tracy LE, Minasian RA, Caterson EJ, Extracellular Matrix and Dermal Fibroblast Function in the Healing Wound, Adv Wound Care (New Rochelle) 5(3) (2016) 119–136. [PubMed: 26989578]

[4]. Xue M, Jackson CJ, Extracellular Matrix Reorganization During Wound Healing and Its Impact on Abnormal Scarring, Adv Wound Care (New Rochelle) 4(3) (2015) 119–136. [PubMed: 25785236]

[5]. Karamanos NK, Theocharis AD, Neill T, Iozzo RV, Matrix modeling and remodeling: A biological interplay regulating tissue homeostasis and diseases, Matrix Biol (2018).

[6]. Ricard-Blum S, Baffet G, Theret N, Molecular and tissue alterations of collagens in fibrosis, Matrix Biol 68–69 (2018) 122–149.

[7]. Herchenhan A, Uhlenbrock F, Eliasson P, Weis M, Eyre D, Kadler KE, Magnusson SP, Kjaer M, Lysyl Oxidase Activity Is Required for Ordered Collagen Fibrillogenesis by Tendon Cells, J Biol Chem 290(26) (2015) 16440–50. [PubMed: 25979340]

[8]. Maki JM, Sormunen R, Lippo S, Kaarteenaho-Wiik R, Soininen R, Myllyharju J, Lysyl oxidase is essential for normal development and function of the respiratory system and for the integrity of elastic and collagen fibers in various tissues, Am J Pathol 167(4) (2005) 927–36. [PubMed: 16192629]

[9]. Chang TC, Yu D, Lee YS, Wentzel EA, Arking DE, West KM, Dang CV, Thomas-Tikhonenko A, Mendell JT, Widespread microRNA repression by Myc contributes to tumorigenesis, Nat Genet 40(1) (2008) 43–50. [PubMed: 18066065]

[10]. Cushing L, Kuang PP, Qian J, Shao F, Wu J, Little F, Thannickal VJ, Cardoso WV, Lu J, miR-29 is a major regulator of genes associated with pulmonary fibrosis, Am J Respir Cell Mol Biol 45(2) (2011) 287–94. [PubMed: 20971881]

[11]. Etoh M, Jinnin M, Makino K, Yamane K, Nakayama W, Aoi J, Honda N, Kajihara I, Makino T, Fukushima S, Ihn H, microRNA-7 down-regulation mediates excessive collagen expression in localized scleroderma, Arch Dermatol Res 305(1) (2013) 9–15. [PubMed: 22965811]

[12]. Fang JH, Zhou HC, Zeng C, Yang J, Liu Y, Huang X, Zhang JP, Guan XY, Zhuang SM, MicroRNA-29b suppresses tumor angiogenesis, invasion, and metastasis by regulating matrix metalloproteinase 2 expression, Hepatology 54(5) (2011) 1729–40. [PubMed: 21793034]

[13]. Ogawa T, Iizuka M, Sekiya Y, Yoshizato K, Ikeda K, Kawada N, Suppression of type I collagen production by microRNA-29b in cultured human stellate cells, Biochem Biophys Res Commun 391(1) (2010) 316–21. [PubMed: 19913496]

[14]. Qin W, Chung AC, Huang XR, Meng XM, Hui DS, Yu CM, Sung JJ, Lan HY, TGF-beta/Smad3 signaling promotes renal fibrosis by inhibiting miR-29, J Am Soc Nephrol 22(8) (2011) 1462–74. [PubMed: 21784902]

[15]. van Rooij E, Sutherland LB, Thatcher JE, DiMaio JM, Naseem RH, Marshall WS, Hill JA, Olson EN, Dysregulation of microRNAs after myocardial infarction reveals a role of miR-29 in cardiac fibrosis, Proc Natl Acad Sci U S A 105(35) (2008) 13027–32. [PubMed: 18723672]

[16]. Roderburg C, Urban GW, Bettermann K, Vucur M, Zimmermann H, Schmidt S, Janssen J, Koppe C, Knolle P, Castoldi M, Tacke F, Trautwein C, Luedde T, Micro-RNA profiling reveals a role for miR-29 in human and murine liver fibrosis, Hepatology 53(1) (2011) 209–18. [PubMed: 20890893]

[17]. Gott VL, Antoine Marfan and his syndrome: one hundred years later, Md Med J 47(5) (1998) 247–52. [PubMed: 9798380]

[18]. Lawrence EJ, The clinical presentation of Ehlers-Danlos syndrome, Adv Neonatal Care 5(6) (2005) 301–14. [PubMed: 16338669]

[19]. Morris CA, Introduction: Williams syndrome, Am J Med Genet C Semin Med Genet 154C(2) (2010) 203–8. [PubMed: 20425781]

[20]. Bornstein P, Diversity of function is inherent in matricellular proteins: an appraisal of thrombospondin 1, J Cell Biol 130(3) (1995) 503–6. [PubMed: 7542656]

[21]. Murphy-Ullrich JE, Sage EH, Revisiting the matricellular concept, Matrix Biol 37 (2014) 1–14. [PubMed: 25064829]

[22]. Calabro NE, Kristofik NJ, Kyriakides TR, Thrombospondin-2 and extracellular matrix assembly, Biochim Biophys Acta 1840(8) (2014) 2396–402. [PubMed: 24440155]

[23]. Stenina-Adognravi O, Invoking the power of thrombospondins: regulation of thrombospondins expression, Matrix Biol 37 (2014) 69–82. [PubMed: 24582666]

[24]. Murphy-Ullrich JE, Iozzo RV, Thrombospondins in physiology and disease: new tricks for old dogs, Matrix Biol 31(3) (2012) 152–4. [PubMed: 22265891]

[25]. Kyriakides TR, Maclauchlan S, The role of thrombospondins in wound healing, ischemia, and the foreign body reaction, J Cell Commun Signal 3(3–4) (2009) 215–25. [PubMed: 19844806]

[26]. Crawford SE, Stellmach V, Murphy-Ullrich JE, Ribeiro SM, Lawler J, Hynes RO, Boivin GP, Bouck N, Thrombospondin-1 is a major activator of TGF-beta1 in vivo, Cell 93(7) (1998) 1159–70. [PubMed: 9657149]

[27]. Isenberg JS, Annis DS, Pendrak ML, Ptaszynska M, Frazier WA, Mosher DF, Roberts DD, Differential interactions of thrombospondin-1, −2, and −4 with CD47 and effects on cGMP signaling and ischemic injury responses, J Biol Chem 284(2) (2009) 1116–25. [PubMed: 19004835]

[28]. Isenberg JS, Jia Y, Fukuyama J, Switzer CH, Wink DA, Roberts DD, Thrombospondin-1 inhibits nitric oxide signaling via CD36 by inhibiting myristic acid uptake, J Biol Chem 282(21) (2007) 15404–15. [PubMed: 17416590]

[29]. Agah A, Kyriakides TR, Lawler J, Bornstein P, The lack of thrombospondin-1 (TSP1) dictates the course of wound healing in double-TSP1/TSP2-null mice, Am J Pathol 161(3) (2002) 831–9. [PubMed: 12213711]

[30]. Rosini S, Pugh N, Bonna AM, Hulmes DJS, Farndale RW, Adams JC, Thrombospondin-1 promotes matrix homeostasis by interacting with collagen and lysyl oxidase precursors and collagen cross-linking sites, Sci Signal 11(532) (2018).

[31]. Kyriakides TR, Zhu YH, Smith LT, Bain SD, Yang Z, Lin MT, Danielson KG, Iozzo RV, LaMarca M, McKinney CE, Ginns EI, Bornstein P, Mice that lack thrombospondin 2 display connective tissue abnormalities that are associated with disordered collagen fibrillogenesis, an increased vascular density, and a bleeding diathesis, J Cell Biol 140(2) (1998) 419–30. [PubMed: 9442117]

[32]. Aimes RT, Quigley JP, Matrix metalloproteinase-2 is an interstitial collagenase. Inhibitor-free enzyme catalyzes the cleavage of collagen fibrils and soluble native type I collagen generating the specific 3/4- and 1/4-length fragments, J Biol Chem 270(11) (1995) 5872–6. [PubMed: 7890717]

[33]. Toth M, Sohail A, Fridman R, Assessment of gelatinases (MMP-2 and MMP-9) by gelatin zymography, Methods Mol Biol 878 (2012) 121–35. [PubMed: 22674130]

[34]. Bein K, Simons M, Thrombospondin type 1 repeats interact with matrix metalloproteinase 2. Regulation of metalloproteinase activity, J Biol Chem 275(41) (2000) 32167–73. [PubMed: 10900205]

[35]. Yang Z, Strickland DK, Bornstein P, Extracellular matrix metalloproteinase 2 levels are regulated by the low density lipoprotein-related scavenger receptor and thrombospondin 2, J Biol Chem 276(11) (2001) 8403–8. [PubMed: 11113133]

[36]. Krady MM, Zeng J, Yu J, MacLauchlan S, Skokos EA, Tian W, Bornstein P, Sessa WC, Kyriakides TR, Thrombospondin-2 modulates extracellular matrix remodeling during physiological angiogenesis, Am J Pathol 173(3) (2008) 879–91. [PubMed: 18688033]

[37]. Agah A, Kyriakides TR, Bornstein P, Proteolysis of cell-surface tissue transglutaminase by matrix metalloproteinase-2 contributes to the adhesive defect and matrix abnormalities in thrombospondin-2-null fibroblasts and mice, Am J Pathol 167(1) (2005) 81–8. [PubMed: 15972954]

[38]. Goddard ET, Hill RC, Barrett A, Betts C, Guo Q, Maller O, Borges VF, Hansen KC, Schedin P, Quantitative extracellular matrix proteomics to study mammary and liver tissue microenvironments, Int J Biochem Cell Biol 81(Pt A) (2016) 223–232. [PubMed: 27771439]

[39]. Tomko LA, Hill RC, Barrett A, Szulczewski JM, Conklin MW, Eliceiri KW, Keely PJ, Hansen KC, Ponik SM, Targeted matrisome analysis identifies thrombospondin-2 and tenascin-C in aligned collagen stroma from invasive breast carcinoma, Sci Rep 8(1) (2018) 12941. [PubMed: 30154546]

[40]. Siegel RC, Biosynthesis of collagen crosslinks: increased activity of purified lysyl oxidase with reconstituted collagen fibrils, Proc Natl Acad Sci U S A 71(12) (1974) 4826–30. [PubMed: 4531019]

[41]. Agah A, Kyriakides TR, Letrondo N, Bjorkblom B, Bornstein P, Thrombospondin 2 levels are increased in aged mice: consequences for cutaneous wound healing and angiogenesis, Matrix Biol 22(7) (2004) 539–47. [PubMed: 14996433]

[42]. Zhang P, Huang A, Ferruzzi J, Mecham RP, Starcher BC, Tellides G, Humphrey JD, Giordano FJ, Niklason LE, Sessa WC, Inhibition of microRNA-29 enhances elastin levels in cells haploinsufficient for elastin and in bioengineered vessels--brief report, Arterioscler Thromb Vasc Biol 32(3) (2012) 756–9. [PubMed: 22095981]

[43]. Honda N, Jinnin M, Kira-Etoh T, Makino K, Kajihara I, Makino T, Fukushima S, Inoue Y, Okamoto Y, Hasegawa M, Fujimoto M, Ihn H, miR-150 down-regulation contributes to the constitutive type I collagen overexpression in scleroderma dermal fibroblasts via the induction of integrin beta3, Am J Pathol 182(1) (2013) 206–16. [PubMed: 23159943]

[44]. Makino K, Jinnin M, Hirano A, Yamane K, Eto M, Kusano T, Honda N, Kajihara I, Makino T, Sakai K, Masuguchi S, Fukushima S, Ihn H, The downregulation of microRNA let-7a contributes to the excessive expression of type I collagen in systemic and localized scleroderma, J Immunol 190(8) (2013) 3905–15. [PubMed: 23509348]

[45]. Alford AI, Golicz AZ, Cathey AL, Reddy AB, Thrombospondin-2 facilitates assembly of a type-I collagen-rich matrix in marrow stromal cells undergoing osteoblastic differentiation, Connect Tissue Res 54(4–5) (2013) 275–82. [PubMed: 23763373]

[46]. Manley E Jr., Perosky JE, Khoury BM, Reddy AB, Kozloff KM, Alford AI, Thrombospondin-2 deficiency in growing mice alters bone collagen ultrastructure and leads to a brittle bone phenotype, J Appl Physiol (1985) 119(8) (2015) 872–81. [PubMed: 26272319]

[47]. Birk DE, Fitch JM, Babiarz JP, Doane KJ, Linsenmayer TF, Collagen fibrillogenesis in vitro: interaction of types I and V collagen regulates fibril diameter, J Cell Sci 95 (Pt 4) (1990) 649–57. [PubMed: 2384532]

[48]. Birk DE, Fitch JM, Babiarz JP, Linsenmayer TF, Collagen type I and type V are present in the same fibril in the avian corneal stroma, J Cell Biol 106(3) (1988) 999–1008. [PubMed: 3346334]

[49]. Chakravarti S, Magnuson T, Lass JH, Jepsen KJ, LaMantia C, Carroll H, Lumican regulates collagen fibril assembly: skin fragility and corneal opacity in the absence of lumican, J Cell Biol 141(5) (1998) 1277–86. [PubMed: 9606218]

[50]. Bonaldo P, Russo V, Bucciotti F, Doliana R, Colombatti A, Structural and functional features of the alpha 3 chain indicate a bridging role for chicken collagen VI in connective tissues, Biochemistry 29(5) (1990) 1245–54. [PubMed: 2322559]

[51]. Takeda U, Utani A, Wu J, Adachi E, Koseki H, Taniguchi M, Matsumoto T, Ohashi T, Sato M, Shinkai H, Targeted disruption of dermatopontin causes abnormal collagen fibrillogenesis, J Invest Dermatol 119(3) (2002) 678–83. [PubMed: 12230512]

[52]. Danielson KG, Baribault H, Holmes DF, Graham H, Kadler KE, Iozzo RV, Targeted disruption of decorin leads to abnormal collagen fibril morphology and skin fragility, J Cell Biol 136(3) (1997) 729–43. [PubMed: 9024701]

[53]. Schonherr E, Witsch-Prehm P, Harrach B, Robenek H, Rauterberg J, Kresse H, Interaction of biglycan with type I collagen, J Biol Chem 270(6) (1995) 2776–83. [PubMed: 7852349]

[54]. Seidler DG, Faiyaz-Ul-Haque M, Hansen U, Yip GW, Zaidi SH, Teebi AS, Kiesel L, Gotte M, Defective glycosylation of decorin and biglycan, altered collagen structure, and abnormal phenotype of the skin fibroblasts of an Ehlers-Danlos syndrome patient carrying the novel

Arg270Cys substitution in galactosyltransferase I (beta4GalT-7), J Mol Med (Berl) 84(7) (2006) 583–94. [PubMed: 16583246]

[55]. Choudhury R, McGovern A, Ridley C, Cain SA, Baldwin A, Wang MC, Guo C, Mironov A Jr., Drymoussi Z, Trump D, Shuttleworth A, Baldock C, Kielty CM, Differential regulation of elastic fiber formation by fibulin-4 and −5, J Biol Chem 284(36) (2009) 24553–67. [PubMed: 19570982]

[56]. Horiguchi M, Inoue T, Ohbayashi T, Hirai M, Noda K, Marmorstein LY, Yabe D, Takagi K, Akama TO, Kita T, Kimura T, Nakamura T, Fibulin-4 conducts proper elastogenesis via interaction with cross-linking enzyme lysyl oxidase, Proc Natl Acad Sci U S A 106(45) (2009) 19029–34. [PubMed: 19855011]

[57]. Sasaki T, Stoop R, Sakai T, Hess A, Deutzmann R, Schlotzer-Schrehardt U, Chu ML, von der Mark K, Loss of fibulin-4 results in abnormal collagen fibril assembly in bone, caused by impaired lysyl oxidase processing and collagen cross-linking, Matrix Biol 50 (2016) 53–66. [PubMed: 26690653]

[58]. Hornstra IK, Birge S, Starcher B, Bailey AJ, Mecham RP, Shapiro SD, Lysyl oxidase is required for vascular and diaphragmatic development in mice, J Biol Chem 278(16) (2003) 14387–93. [PubMed: 12473682]

[59]. Maki JM, Rasanen J, Tikkanen H, Sormunen R, Makikallio K, Kivirikko KI, Soininen R, Inactivation of the lysyl oxidase gene Lox leads to aortic aneurysms, cardiovascular dysfunction, and perinatal death in mice, Circulation 106(19) (2002) 2503–9. [PubMed: 12417550]

[60]. Levene CI, Structural requirements for lathyrogenic agents, J Exp Med 114 (1961) 295–310. [PubMed: 13761342]

[61]. Galan M, Varona S, Guadall A, Orriols M, Navas M, Aguilo S, de Diego A, Navarro MA, Garcia-Dorado D, Rodriguez-Sinovas A, Martinez-Gonzalez J, Rodriguez C, Lysyl oxidase overexpression accelerates cardiac remodeling and aggravates angiotensin II-induced hypertrophy, FASEB J (2017).

[62]. Adam O, Theobald K, Lavall D, Grube M, Kroemer HK, Ameling S, Schafers HJ, Bohm M, Laufs U, Increased lysyl oxidase expression and collagen cross-linking during atrial fibrillation, J Mol Cell Cardiol 50(4) (2011) 678–85. [PubMed: 21215756]

[63]. Vanacore R, Ham AJ, Voehler M, Sanders CR, Conrads TP, Veenstra TD, Sharpless KB, Dawson PE, Hudson BG, A sulfilimine bond identified in collagen IV, Science 325(5945) (2009) 1230–4. [PubMed: 19729652]

[64]. Bhave G, Cummings CF, Vanacore RM, Kumagai-Cresse C, Ero-Tolliver IA, Rafi M, Kang JS, Pedchenko V, Fessler LI, Fessler JH, Hudson BG, Peroxidasin forms sulfilimine chemical bonds using hypohalous acids in tissue genesis, Nat Chem Biol 8(9) (2012) 784–90. [PubMed: 22842973]

[65]. Colon S, Bhave G, Proprotein Convertase Processing Enhances Peroxidasin Activity to Reinforce Collagen IV, J Biol Chem 291(46) (2016) 24009–24016. [PubMed: 27697841]

[66]. Akagawa M, Suyama K, Mechanism of formation of elastin crosslinks, Connect Tissue Res 41(2) (2000) 131–41. [PubMed: 10992159]

[67]. Cushing L, Kuang P, Lu J, The role of miR-29 in pulmonary fibrosis, Biochem Cell Biol 93(2) (2015) 109–18. [PubMed: 25454218]

[68]. Maurer B, Stanczyk J, Jungel A, Akhmetshina A, Trenkmann M, Brock M, Kowal-Bielecka O, Gay RE, Michel BA, Distler JH, Gay S, Distler O, MicroRNA-29, a key regulator of collagen expression in systemic sclerosis, Arthritis Rheum 62(6) (2010) 1733–43. [PubMed: 20201077]

[69]. Ulrich V, Rotllan N, Araldi E, Luciano A, Skroblin P, Abonnenc M, Perrotta P, Yin X, Bauer A, Leslie KL, Zhang P, Aryal B, Montgomery RL, Thum T, Martin K, Suarez Y, Mayr M, Fernandez-Hernando C, Sessa WC, Chronic miR-29 antagonism promotes favorable plaque remodeling in atherosclerotic mice, EMBO Mol Med 8(6) (2016) 643–53. [PubMed: 27137489]

[70]. Hill RC, Calle EA, Dzieciatkowska M, Niklason LE, Hansen KC, Quantification of extracellular matrix proteins from a rat lung scaffold to provide a molecular readout for tissue engineering, Mol Cell Proteomics 14(4) (2015) 961–73. [PubMed: 25660013]

[71]. Dennis G Jr., Sherman BT, Hosack DA, Yang J, Gao W, Lane HC, Lempicki RA, DAVID: Database for Annotation, Visualization, and Integrated Discovery, Genome Biol 4(5) (2003) P3. [PubMed: 12734009]

[72]. Xia J, Sinelnikov IV, Han B, Wishart DS, MetaboAnalyst 3.0--making metabolomics more meaningful, Nucleic Acids Res 43(W1) (2015) W251–7. [PubMed: 25897128]

[73]. Xia J, Wishart DS, Web-based inference of biological patterns, functions and pathways from metabolomic data using MetaboAnalyst, Nat Protoc 6(6) (2011) 743–60. [PubMed: 21637195]

[74]. Sims TJ, Avery NC, Bailey AJ, Quantitative determination of collagen crosslinks, Methods Mol Biol 139 (2000) 11–26. [PubMed: 10840774]

[75]. Nemkov T, D'Alessandro A, Hansen KC, Three-minute method for amino acid analysis by UHPLC and high-resolution quadrupole orbitrap mass spectrometry, Amino Acids 47(11) (2015) 2345–57. [PubMed: 26058356]

[76]. Yamauchi M, Shiiba M, Lysine hydroxylation and cross-linking of collagen, Methods Mol Biol 446 (2008) 95–108. [PubMed: 18373252]

[77]. Subramaniam M, Saffaripour S, Van De Water L, Frenette PS, Mayadas TN, Hynes RO, Wagner DD, Role of endothelial selectins in wound repair, Am J Pathol 150(5) (1997) 1701–9. [PubMed: 9137094]

Highlights

Extracellular matrix (ECM) solubility depends, in part, on the extent of collagen crosslinking by enzymes such as lysyl oxidase (LOX), however, the regulation of this enzyme is not fully understood

Here we show that LOX levels are altered in cells and skin of thrombospondin 2 (TSP2) KO mice and that this alteration contributes to reduced crosslinking and increased ECM solubility

These properties were assessed by quantitative proteomics and biochemical analysis of crosslinks, which revealed alterations in ECM composition and crosslinking

To probe pathways involved in the regulation of LOX, we explored the participation of microRNAs (miRs) and discovered that TSP2 influences levels of miR-29

Thus, we demonstrate a previously undescribed connection between TSP2, ECM production, and LOX that involves regulation of miR-29, ultimately having significant implications on the formation of skin ECM

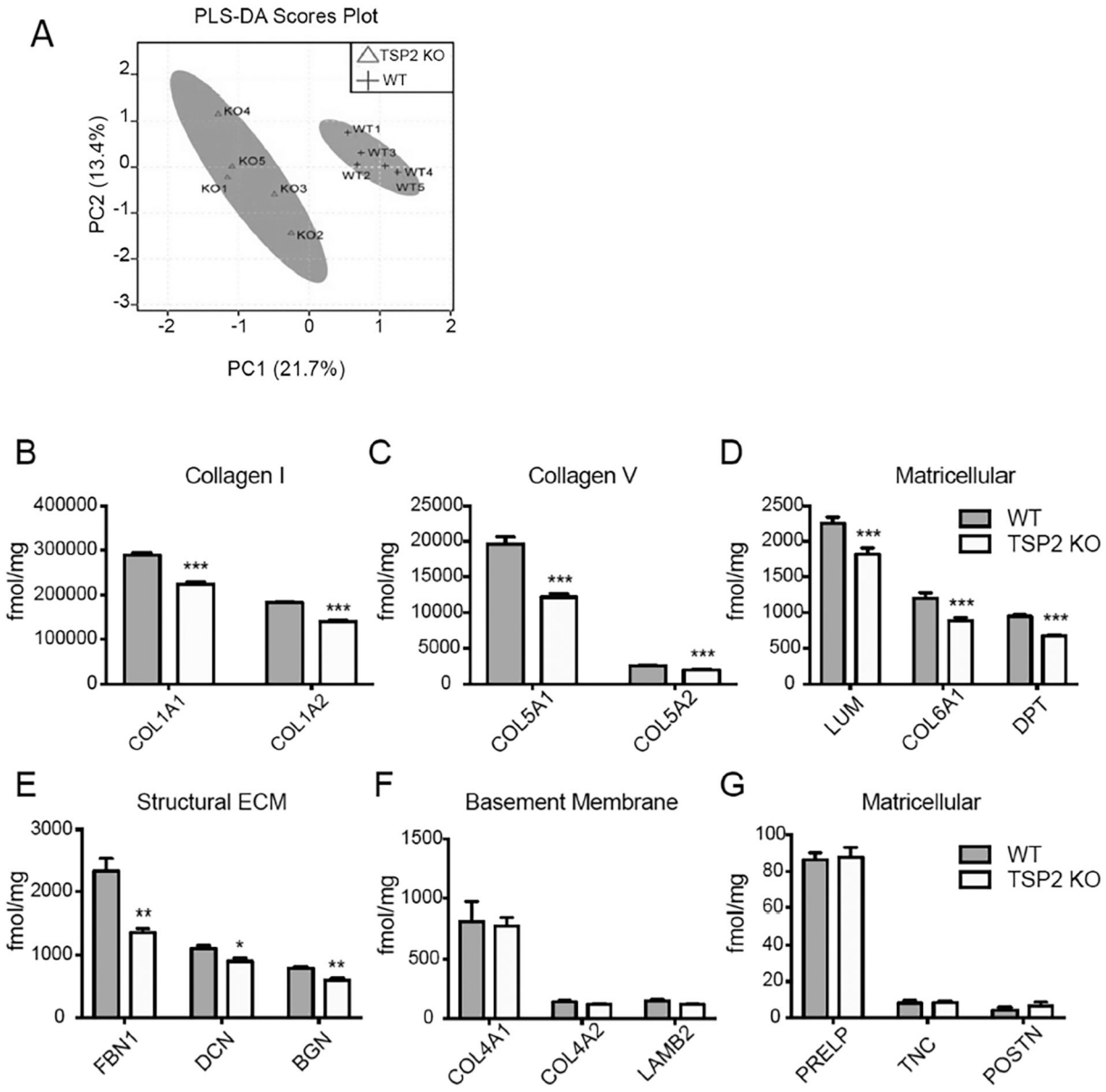

Fig. 1.

TSP2 KO skin possesses a unique ECM protein profile highlighted by a decrease in fibrillar collagens, matricellular proteins, and structural ECM proteins. (A) Multivariate analysis of quantitative LC-MS/MS data from WT and TSP2 KO mice skin reveals that TSP2 KO skin possesses a unique ECM profile as demonstrated by the evident separated clustering in the PLS-DA plot. (B-E) Furthermore, quantitative LC-MS/MS analysis shows a significant decrease in both the α1 and α2 chains of collagen I and the α1 chain of V, along with a decrease in matricellular proteins (lumican, collagen VI, dermatopontin) and structural ECM proteins (fibrillin-1, decorin, and biglycan) in TSP2 KO skin. However, there is not a global decrease in ECM proteins, as levels of major basement membrane proteins collagen IV and laminin (F), along with matricellular proteins prolargin, tenascin, and periostin (G) remain

similar between WT and TSP2 KO skin. Data is represented as mean ± SEM. p*<0.05, p**<0.01, p***<0.005. N=5 mice per group.

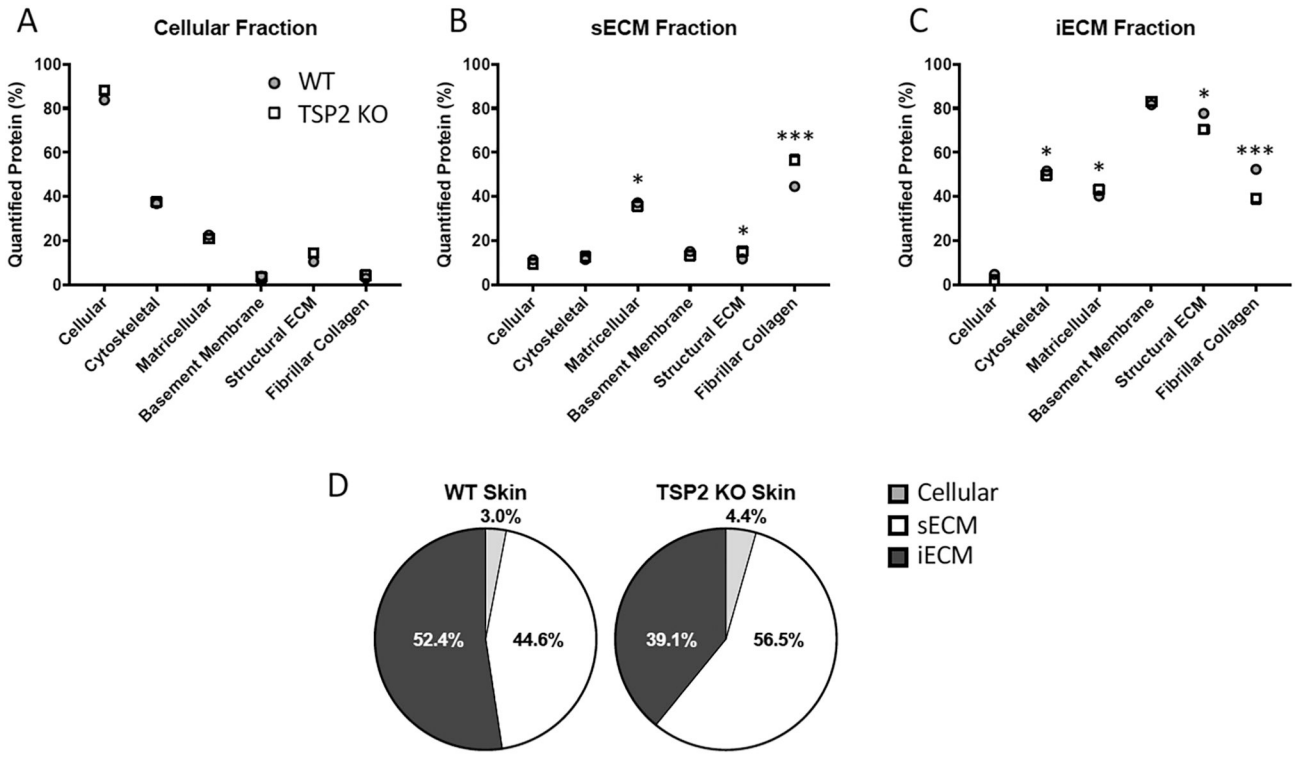

Fig. 2.

TSP2 KO skin displays greater fibrillar collagen and structural ECM protein solubility. Quantitative LC-MS/MS analysis of WT and TSP2 KO skin after multi-step fractionation reveals no change in protein solubility within the cellular fraction (A). However, there is a 12.0 % increase in fibrillar collagen solubility in the soluble ECM (sECM) fraction of TSP2 KO skin (B,D), followed by a corresponding decrease of fibrillar collagen in the insoluble ECM (iECM) fraction of TSP2 KO skin. A similar trend is seen (B,C) with structural ECM proteins. p*<0.05, p***<0.005 for N=5 mice per group.

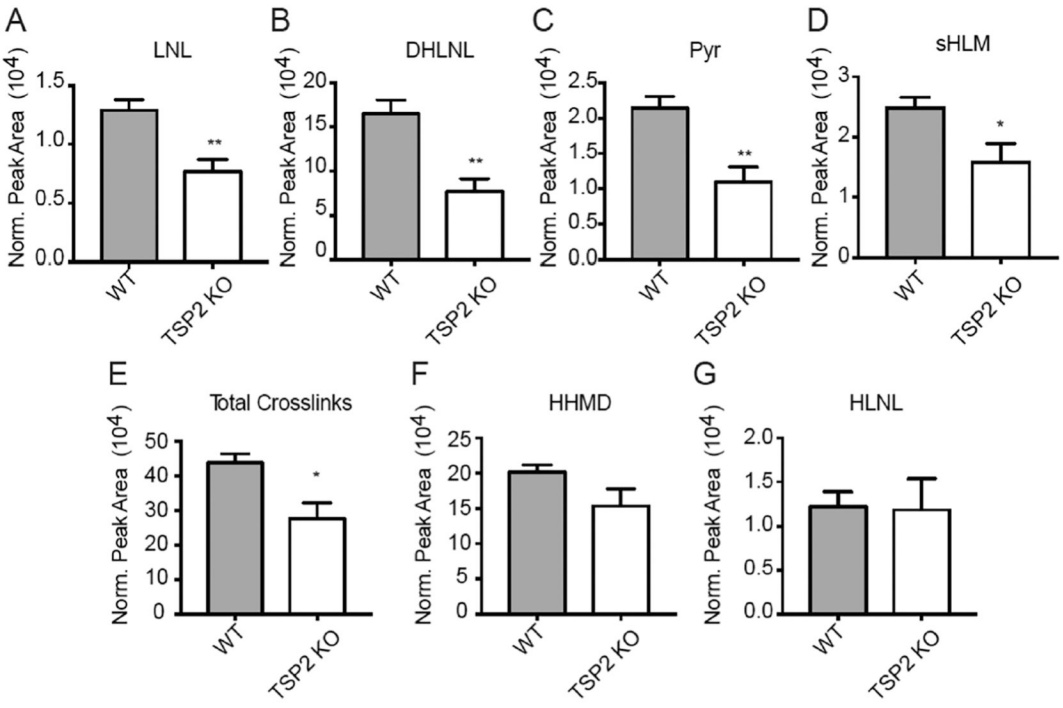

Fig. 3.

TSP2 KO skin contains less collagen crosslinks. HPLC analysis reveals (A,B) LOX-mediated divalent crosslinks LNL and HLNL, along with (C) trivalent crosslink Pyr, are significantly lower in TSP2 KO skin. Additionally, (D) levels of the collagen IV crosslink sHLM are significantly lower in TSP2 KO skin. Collectively, these changes result in a significant decrease of total crosslinks in the TSP2 KO skin (E). However, there is not a global decrease in crosslinks as HLNL and HHMD crosslinks are not significantly lower (F,G). Data is represented as mean ± SEM. p*<0.05, p**<0.01. N=5 mice per group

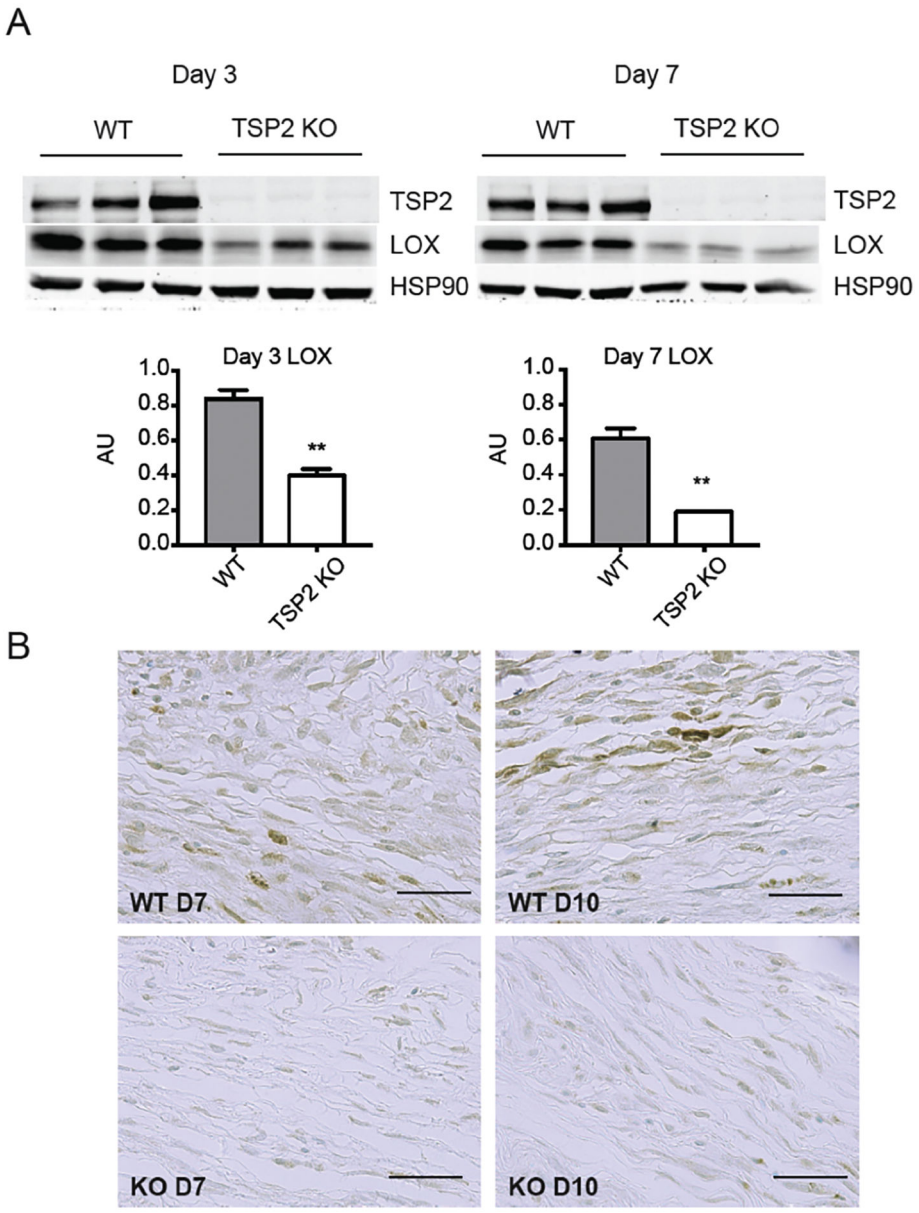

Fig. 4.

Reduced levels of LOX protein in TSP2 KO mice and DF. (A) Western blot analysis of WT and TSP2 KO DF lysates collected from DF cultured for 3 and 7 days in ascorbic acid induced ECM production conditions indicates lower LOX protein levels at both timepoints. HSP90 is used as loading control. Densitometry from 3 independent experiments is shown on the bottom. A.U., arbitrary units. Data is represented as mean ± SEM. **p<0.01. (B-C) Immunohistochemistry of full dermal thickness wounds harvested at days 7 and 10 post-injury indicates that, in comparison to WT, TSP2 KO wounds display decreased LOX staining. Immunoreactive cells are identified by black arrows. (Magnification: 20X) N=5 mice per group.

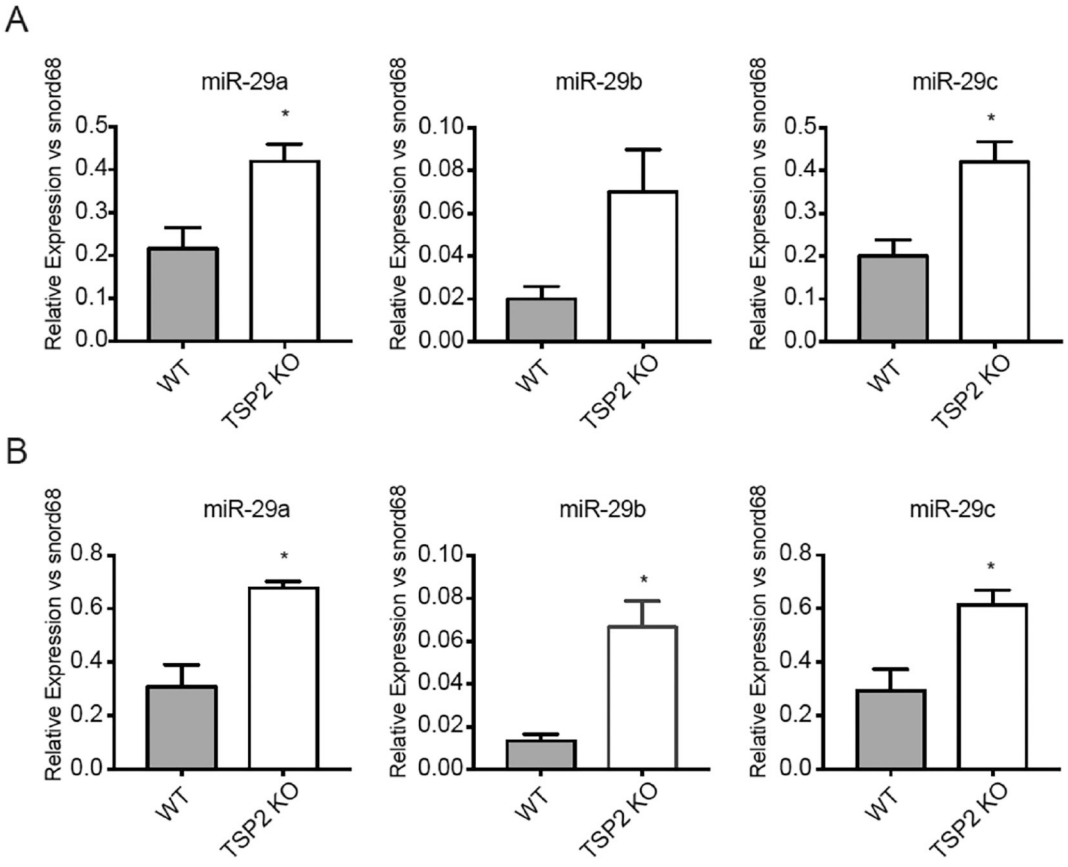

Fig. 5.

Increased levels of miR−29 expression in TSP2 KO dermal fibroblasts. qPCR analysis of miR−29a, −29b and −29c at day 3 (A) and day 7 (B) timepoints of ascorbic acid induced ECM production indicates that levels of miR−29a and −29c are significantly higher in TSP2 KO DF at day 3, and that miR−29a, −29b, and −29c levels are all significantly higher in TSP2 KO DF at day 7. Data is represented as mean ± SEM. p*<0.05. N=6 independent experiments.

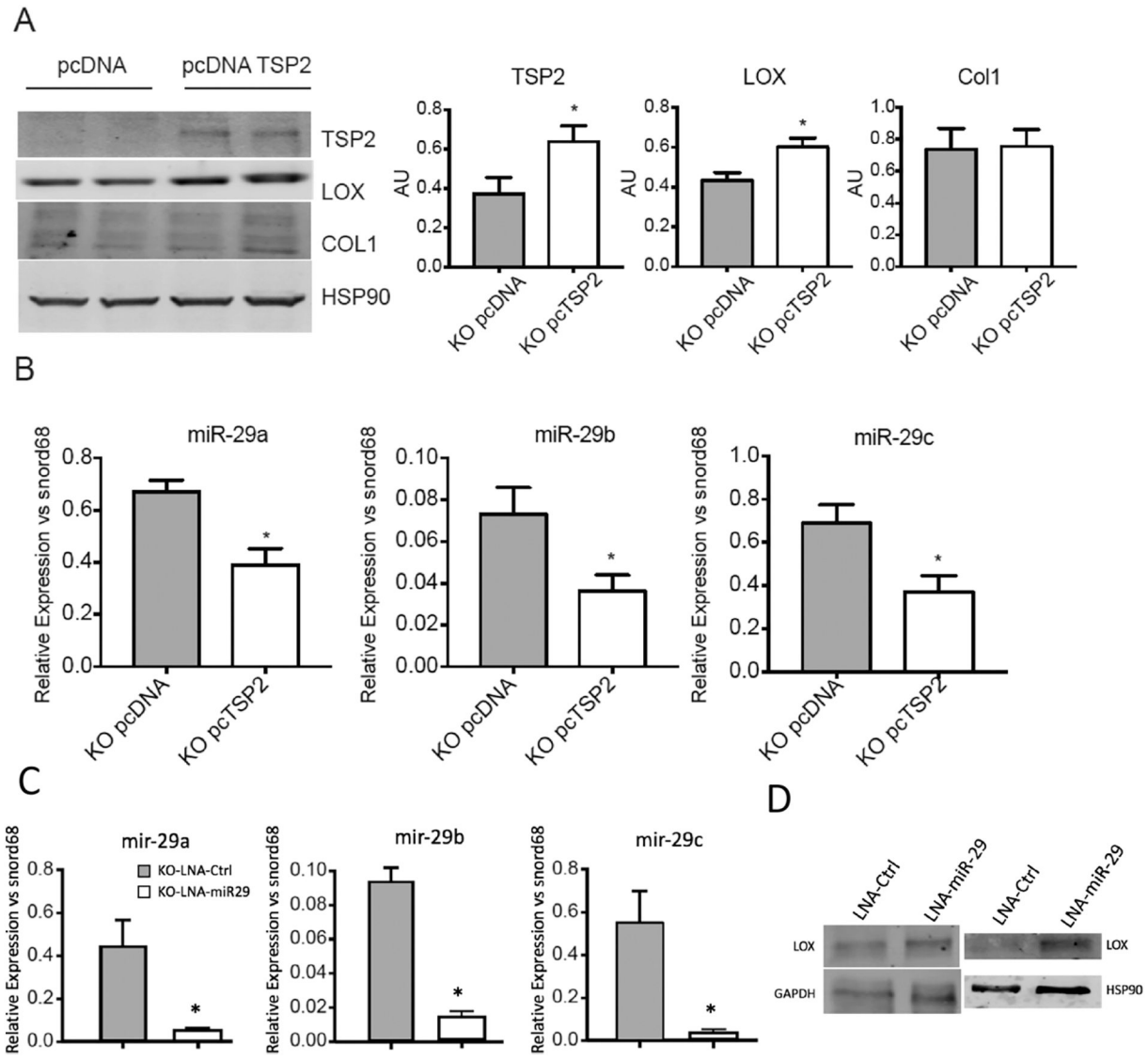

Fig. 6.

Rescue of TSP2 or reduction of miR-29 in TSP2 KO DF leads to increased LOX. TSP2 KO cells were transfected with 0.5 μg of pcDNA or pcDNA TSP2 in order to rescue loss of TSP2. (A) Western blot analysis of TSP2 KO cells transfected with pcDNA TSP2 reveals a significant increase in LOX 48 hours post-transfection. HSP90 is used as loading control. Densitometry from 3 independent experiments is shown on the right. A.U., arbitrary units. Data is represented as mean ± SEM. *p<0.05. (B) qPCR analysis of TSP2 KO cells transfected with pcDNA TSP2 demonstrates a significant decrease of miR-29a, −29b and −29c levels 48 hours post-transfection. Data is represented as mean ± SEM. p*<0.05. N=6 independent experiments. (C) TSP2 KO cells were treated with LNA-control or LNA-miR-29 for 48 hrs in order to reduce miR-29 levels. All miR-29 isoforms were reduced by LNA-miR-29 treatment. Data is represented as mean ± SEM. p*<0.05. N=4 independent experiments. (D) Western blot analysis of TSP2 KO cells revealed an increase in LOX 48

hours post treatment with LNA-miR-29. GAPDH and HSP90 were used as loading controls. Blots are representative of two independent experiments.

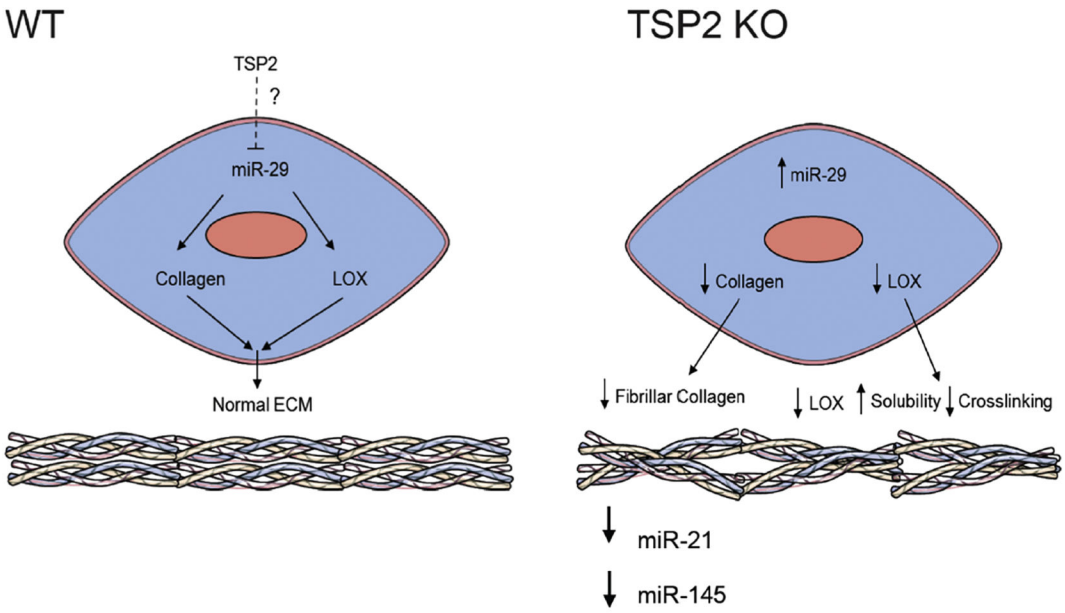

Fig. 7.

Role of TSP2 in modulating the ECM. In the WT environment, a balance exists between miR-29, collagen, and LOX levels that allows for the production of a normally assembled and crosslinked ECM. However, in a TSP2 KO environment, there is an increase in miR-29 expression, along with a decrease in fibrillar collagens and LOX-mediated fibrillar collagen crosslinking, leading to altered ECM assembly and composition. This data demonstrates a novel link between TSP2, collagen, LOX, and miR-29 that is regulated by the presence or absence of TSP2 in the extracellular environment, forming a feedback loop between cells and its ECM substrate.